

MIREA – An on-line real time solution to check the electrical quality of anodes

**Guillaume Léonard¹, Ameline Bernard², Yann El Ghaoui³, Marc Gagnon⁴, Patrick Coulombe⁵,
Gontran Bourque⁶ and Stéphane Gourmaud⁷**

1. R&D project leader, Arvida Research and Development Center, Rio Tinto

2. Carbon technology consultant, Smelter Technology and R&D, Rio Tinto

3. Carbon and Environment domain director, Smelter Technology and R&D, Rio Tinto

4. Technical advisor, Aluminerie Alouette

5. Continuous Improvement and Technology Development manager, Aluminerie Alouette

6. Automation analyst, Aluminerie Alouette

7. R&D project leader, Fives ECL

Corresponding author: yann.elghaoui@riotinto.com

Abstract

Fives ECL has introduced on the market a new tool called MIREA. This tool is used to measure the quality of anodes, which will be used in pot lines for the production of primary aluminium. The system is based on a non-destructive measurement of the anode electrical resistance imitating the current distribution of an anode in use. It is inspired by the work undertaken by Chollier-Brym et al. [1] and numerous measurement campaigns carried out under the supervision of Rio Tinto/AP Technology™ experts since 2012. This technology is now under commissioning in a mature anode plant (Alouette Smelter in Sept-Îles, Québec), who gave a strong support in the industrialization process. MIREA has many advantages compared to the traditional core sampling process. It helps the carbon plant of a primary aluminium smelter to control more effectively its anode production process; all anodes are measured in real time. It also helps the Reduction sector to identify and reject anodes having internal cracks, which could lead to premature failure of the anodes in use or unacceptable energy consumption. Globally, the use of MIREA helps reducing carbon waste and increasing pot performance.

Keywords: Carbon resistivity; Anode resistance; Anode voltage drop; Real time measurement.

1. Introduction

Anode electrical resistance is increasingly recognized as a key parameter for pot operation. Generally, evaluation of the electrical performance of an anode population is based on weekly resistivity averages taken on a limited number of anode core samples. Few anodes are cored weekly since this operation is time-consuming and destructive. Core sampling also provides limited information on the spatial variability within an anode. For example, cracks in a specific anode section could remain undetected due to the absence of sampling in that specific region. Furthermore, resistivity measurements in smelters are typically based on the ISO standard 11713 [2]. With this standard, the current distribution in the core sample is almost ideal (top-bottom current distribution) and cannot take into account the specific current distribution near the stub hole vicinity [1]. Indeed, current distribution is mostly horizontal in this region of the anode.

Consequently, anode coring methods cannot provide an accurate assessment of the electrical performance of an anode population due to the insufficient number of samples taken every week and the lack of spatial resolution. Furthermore, resistivity results are usually obtained weeks after the introduction of the anode in the pot. Therefore, technical teams in smelters cannot take sound decisions or immediate corrective actions.

For the above-mentioned reasons, an instantaneous and non-destructive R&D device was developed by Rio Tinto to evaluate the contribution of different anode regions on the anodic electrical resistance. The acronym for MIREA is derived from a French translation “Instantaneous Measurement of Anodic Electrical Resistance”. The R&D device was initially introduced by Chollier-Brym et al. [1]. In their paper, comparisons were made between the MIREA measures and an intensive anode coring campaign. It was shown that the trend between the MIREA measures and the core samples corresponded in the lower part of the anode. However, the coring samples underestimated the resistivity in the upper part of the anode due to the top-to-bottom current distribution of the core sample, as explained earlier. They also investigated the influence of two forming processes (press and vibroformer) on the anode electrical resistance. This work was followed by a second paper summarizing six MIREA campaigns held at different anode plants around the world [3]. More than 600 anodes were characterized. These campaigns highlighted resistance heterogeneity problems such as highly resistive tops and helped detect non-optimized vibroformers in some anode plants. For example, an important gap of apparent resistivity ($\sim 17 \mu\Omega\text{m}$), in the top anode section, was observed between two carbon plants producing a similar anode format. This resistivity difference had never been detected before due to the absence of core samples in this specific region. It should be noted that an important resistivity, in the top section of the anode, will penalize the anode voltage drop throughout the entire reduction cycle since this anode section will always be present.

Following the success of the MIREA campaigns, an industrial version was developed in collaboration with Rio Tinto/AP Technology™ experts, Fives ECL and Alouette Smelter (Sept-Îles, Québec). The first industrial version of this technology is now under commissioning at Alouette. All anodes can be measured in real time to provide not only an electrical resistance estimate of the anode population, but the exact resistance and dispersion of the population itself. Alouette is on track to efficiently characterize its anode production process. Algorithms are now being set up to identify and reject anodes having critical deficiencies leading to premature anode failures in the pots or leading to excessive energy consumption.

This paper presents a first glimpse of the capacity of this on-line process technology by summarizing the resistance measurements of more than 10 000 anodes produced between June and August 2015. A description of the industrial MIREA device is presented in the first section of this paper. This section is followed by an analysis of individual anodes and a statistical evaluation of the Alouette anode population. Finally, a simple straightforward rejection algorithm is proposed as an initial step to identify anodes having critical deficiencies.

2. Description of the industrial MIREA

2.1. MIREA integration in the process chain

Alouette integrated the industrial MIREA device on their baked anode conveyor servicing two anode baking furnaces in the anode handling area. Consequently, every baked anode produced by the two baking furnaces passes through the MIREA device for measurement or bypass. Anodes rejected, based on the MIREA results, are then redirected to an alternative conveyor to be withdrawn from the production.

The MIREA device was designed to handle anodes exiting the anode baking furnaces at temperatures up to 400 °C. However, it was found that the MIREA is exposed to anode

temperatures varying between 25 and 250 °C. This temperature interval is lower than the maximal intended limit of the device. Temperature corrections are applied to the raw MIREA measurements, thus providing a basis of comparison between the anodes measured at different temperatures. The reference temperature can be set to room temperature, to allow comparison of resistivity measurements with core samples, or set to pot temperature, to provide an estimate of the anodic voltage drop in service.

The industrial device was also designed to reliably achieve an anode measurement per minute. The measurement sequence includes the following chronological steps: position the baked anode into the device, introduce current devices into the anode stub holes, measure the anode voltage drop, withdraw current devices from stub holes, and remove anode from the MIREA. At the Alouette Smelter, at top production rates, the MIREA was able to complete measurement sequences in time intervals varying between 60 to 66 seconds. This cycle time measurement was achieved for more than 15% of the population. At other times, this measurement rate was not required since the production rate was lower.

It should be noted that the MIREA device is completely automated and requires limited maintenance. Anodes with excessive irregular dimensions are automatically bypassed and can be rejected, if needed. For example, this situation could arise when a thick layer of packing coke (more than 1 cm) is agglomerated to the anode surface.

2.2. Measurement principles

The MIREA device shown in Figure 1 focusses on the critical role of the stub holes area to the anode electrical resistance. Thus, it allows a characterization of the anode electrical properties under the same current flow patterns as those found during electrolysis. The device replicates the anodic current distribution using stub hole devices imitating the standard anodic rodding. These stub hole devices establish an electrical connection to the anode, thereby allowing the passage of an electric current. The devices were designed to adapt to irregular stub hole shapes such as holes with missing flutes or ellipsoid geometries. The MIREA device includes independent power sources for each stub hole. The electric circuit is completed with a carpet in contact with the anode bottom surface. A voltmeter is used to establish a voltage drop map of the anode side surfaces. Voltage drops are measured between reference points (H_0) located on the top of the anode and at predefined positions on the anode surface.



Figure 1. Industrial MIREA in Fives ECL warehouse.

These voltage drop measures are taken following a predefined template consisting of four columns of measures (C_1 to C_4) with seven position levels (H_1 to H_7). As illustrated in Figure 2, these columns are located between the stub holes. A total of 28 “mV” measures are taken for each anode. This measurement template is considered a good trade-off between the operating mode of the device, the measurement cadence and the anode representativeness.

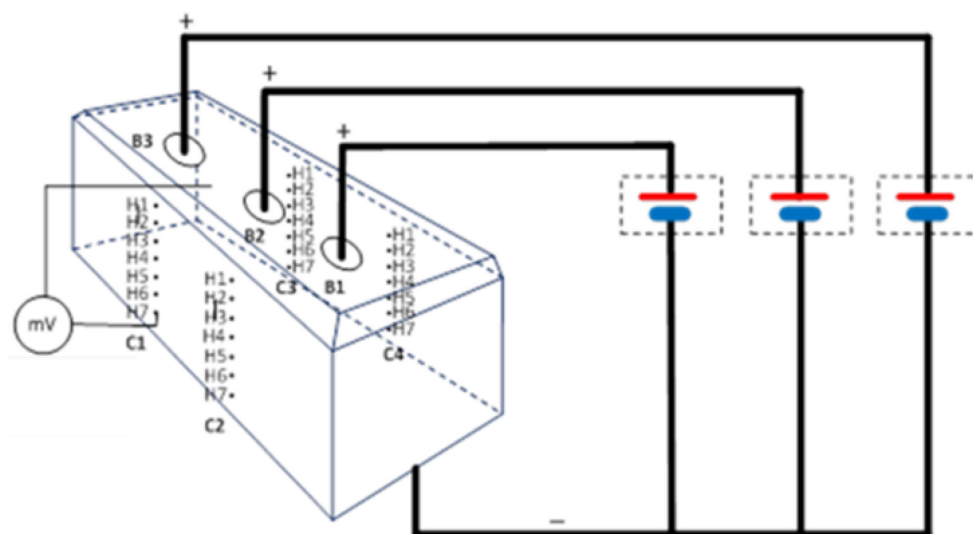


Figure 2. MIREA measurement position template.

2.3. Conversion of raw data into apparent resistivity

The millivolt measurements of the anode surface can be converted into apparent resistivity values [1]. This transformation is not required for a carbon plant producing the same anode format. Indeed, “mV” measurements are sufficient to evaluate the process disturbances with time, and measure the performance of individual anode for rejection purposes. However, this data transformation provides a physical grasp of the MIREA to standard resistivity units and can

allow comparisons between different anode formats. Comparisons between carbon plants can be found in the second MIREA paper summarizing six campaigns [3]. Numerical simulations modeling the electrical potential drop on the anode surface are used for this unit conversion. These simulations are based on the anode blueprint, use a constant resistivity value and match the current intensity target of the MIREA. A simulation of a generic anode format is illustrated in Figure 3.

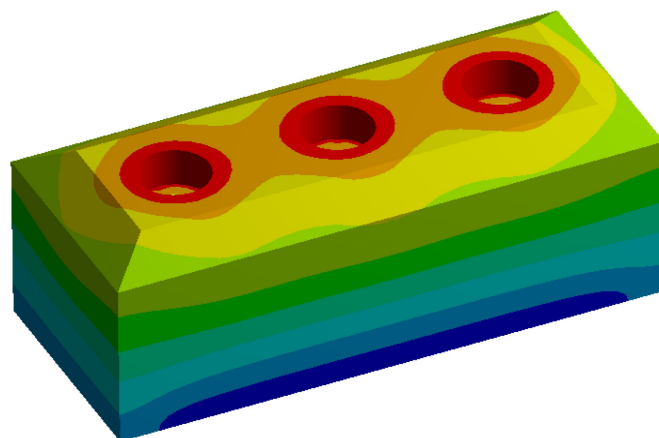


Figure 3. Numerical simulation of a generic anode format showing voltage drop on the anode surface (Red: High voltage value, Blue: Low voltage value).

To perform a resistivity conversion, it is assumed that the resistivity of an anode slice section, $\rho(S_i)$, is proportional to the slice voltage drop, $\Delta V(S_i)$, measured between the slice boundaries H_{i-1} and H_i (Figure 2). The proportionality factor of this relation is the ratio between the simulation resistivity (ρ_s) and the simulated voltage drop of S_i , $\Delta V_s(S_i)$:

$$\rho(S_i) = \frac{\rho_s}{\Delta V_s(S_i)} \Delta V(S_i) \quad (1)$$

$\rho(S_i)$ Apparent resistivity of section S_i ($\mu\Omega\text{m}$);

ρ_s Simulation resistivity ($\mu\Omega\text{m}$);

$\Delta V(S_i)$ Voltage drop of S_i (mV);

$\Delta V_s(S_i)$ Simulated voltage drop of S_i (mV).

It must be noted that this assumption is valid if the current distribution in real life anode is similar to that of the simulated case. However, some biases are always present between the real and simulated current distribution due to the heterogeneity of the real life anode. Therefore, this document continually refers to an apparent resistivity value, when presenting resistivity data.

3. Results and discussion

3.1. MIREA fingerprint of Alouette individual anodes

Figures 4 and 5 show the “mV” fingerprints collected by the MIREA device. Figure 4 illustrates the cumulated voltage drop between the reference point (H_0) and seven anode position levels, (H_i) while Figure 5 presents the voltage drop according to different sliced sections of an anode (S_i). All “mV” data are normalized to a temperature of 25 °C. In Figures 4 and 5, each point represents an average of the measurements at the specified anode position level (H_i) for the four

columns. This average hides some variability between columns, however, it allows a simple visual representation of the anode general behaviour which can then be compared to other anodes. Other representations can also be used such as the one presented in Figure 6. In this case, deviations from an averaged anode profile are highlighted in red for all 28 “mV” measurement positions.

Figures 4 and 5 include four anodes considered as mediocre and four other anodes considered as fair. The average fingerprint of the population is also included for comparison purposes in both figures. The anodes presented in the figures were randomly selected based on a principal component analysis (PCA) using the Mahalanobis distance as a discrimination parameter. This multivariate approach will be further discussed in Section 3.3.

In Figures 4 and 5, anodes having resistance defects are identified with a “red fingerprint”. As it can be seen, “red fingerprint” anodes deviate from the “fair” anode population represented as “blue fingerprints”. These deviations indicate the presence of anode defects at the corresponding position level. In Figure 5, the representation of “mV” data is interesting since it allows a much easier visual detection of anomalies such as “sawtooth” patterns, when compared to the cumulative “mV” representation shown in Figure 4.

In Figure 4, it can be observed that the voltage drop distribution in the upper anode section (H_1) is narrower than that of the lower anode section (H_7). This phenomenon is explained by the accumulation of resistance artifacts along the anode height. Figure 4 also represents qualitatively the expected anode voltage drop during the reduction cycle. The abscissa position level (H_i) can, in fact, be associated to the reduction cycle time frame. Indeed, H_7 can be linked to an approximation of the voltage drop during the introduction of anodes in the pot, whereas a position level between H_2 and H_3 is associated with spent anode voltage drop. The lifetime anode voltage drop can, therefore, be estimated by averaging the voltage drop between two position levels representing the full anode and the spent anode. To do so, the MIREA “mV” raw data must be normalized at the pot temperature and at the anode amperage level in the pot line.

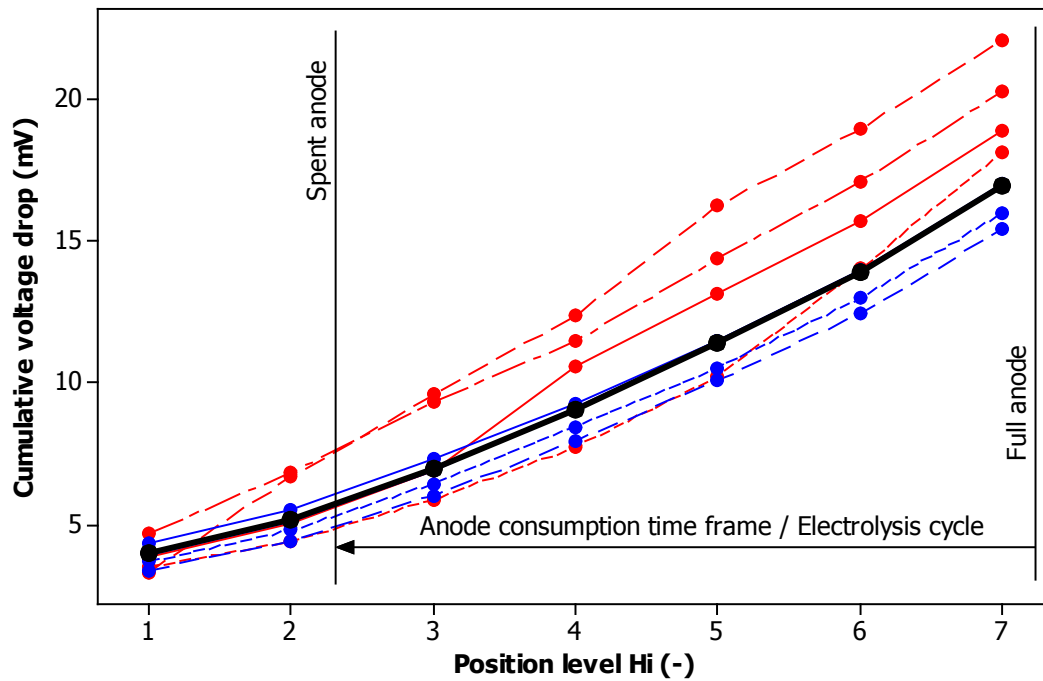


Figure 4. MIREA cumulated “mV” measures as a function of position levels (H_i). In blue: fair anodes; in red: mediocre anodes; in black: population average.

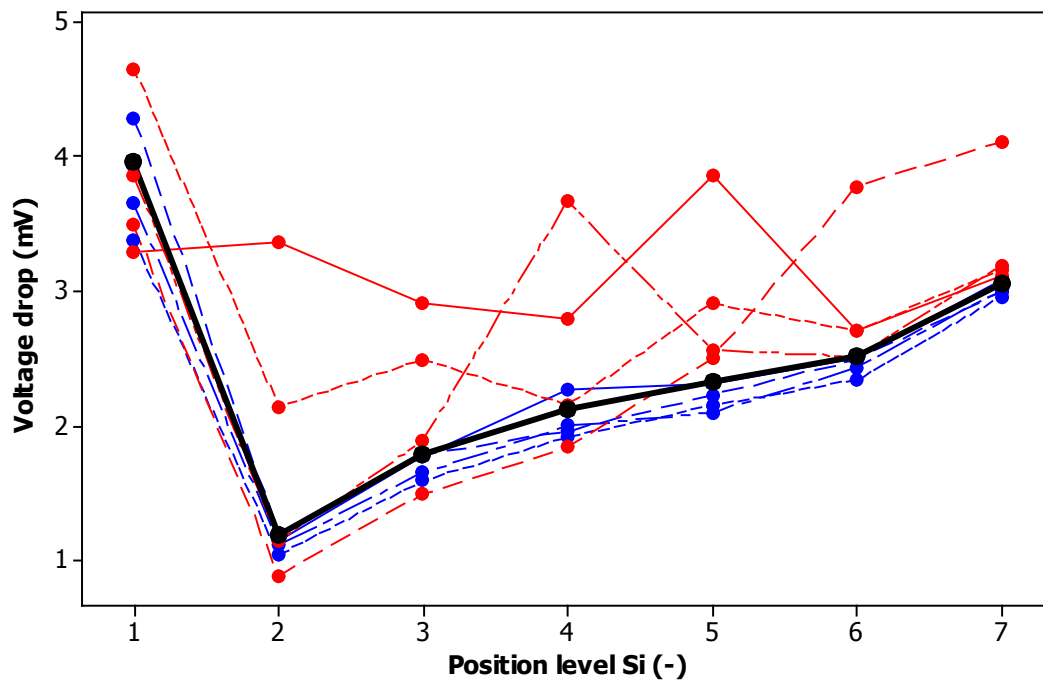


Figure 5. MIREA sliced “mV” measures as a function of position levels (S_i). In blue: fair anodes; in red: mediocre anodes; in black: population average.

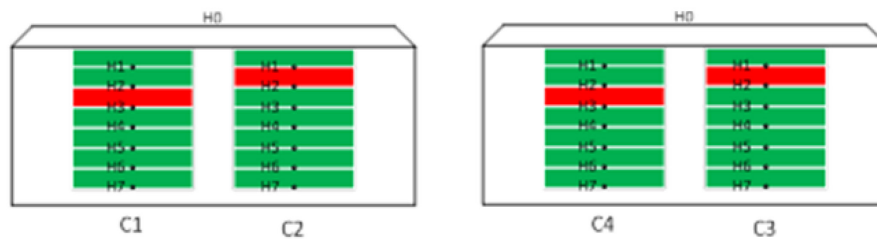


Figure 6. Anode representation of the MIREA raw data. In red: deviation from averaged profile.

Figure 7 presents the apparent resistivity translation of anodes presented in Figures 4 and 5. As previously mentioned, this is done to provide a physical grasp of the “mV” data. The points found on each fingerprint represent the apparent resistivity of an anode sliced section (S_i). As in Figure 5, the same “sawtooth” patterns are observed. Some of them are exacerbated due to the unit conversion and calibration in accordance with the voltage drop model. As previously indicated, these artifacts are associated to the presence of significant internal cracks, which disturb the current distribution around these layers. It must be noted that the presence of a very low resistivity value, such as the one highlighted in Figure 7, is not associated to a good resistivity value, but to an anodic defect, which disrupts the current intensity in this layer. The current distribution of the actual anode is not equivalent to the simulated case for this section. It is believed, in this case, that there is a preferred pathway that does not pass in the vicinity of the four “mV” probes on slice S_2 , thereby reducing the current intensity in this specific region. However, the presence of these deviations, from normality, clearly indicates important anode defects.

Alouette averaged resistivity fingerprint follows a relatively constant pattern along the position level S_i . As for other carbon plants, a generally decreasing pattern along the anode height was observed from previous campaigns with the R&D MIREA [3].

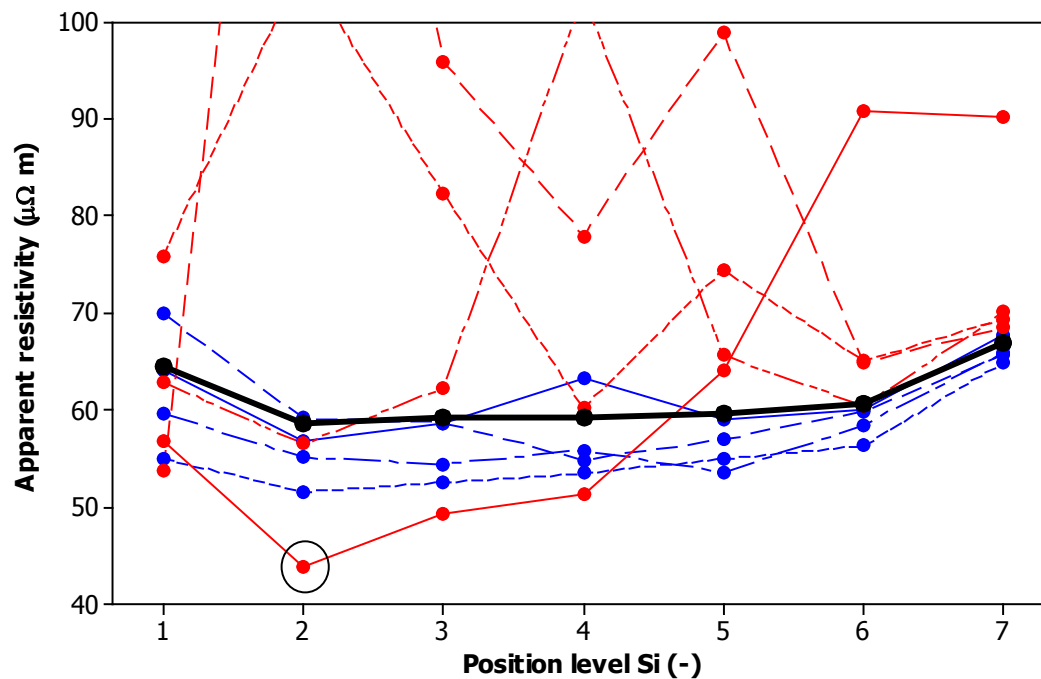


Figure 7. Anode apparent resistivity profile for anodes presented in Figure 5 for Slices S_i . In blue: fair anodes; in red: mediocre anodes; in black: population average.

3.2. Alouette distribution based on the industrial MIREA

As for the variability of populations, Figure 8 illustrates the global apparent resistivity distribution of the Alouette anode population. This frequency distribution was built using the ΔV_{H0-H7} voltage drop parameter, which estimates the apparent resistivity of the entire anode using the calibration model presented in Figure 3. It must be mentioned that due to this treatment, the presence of punctual defects with the averaging actions on columns and slices were hidden. The Alouette population showed a non-normal bell shape distribution with a certain degree of skewness. This distribution pattern was expected as there is a physical limit to produce low resistive anodes. However, upper resistivity anodes are not constrained and can reach high values.

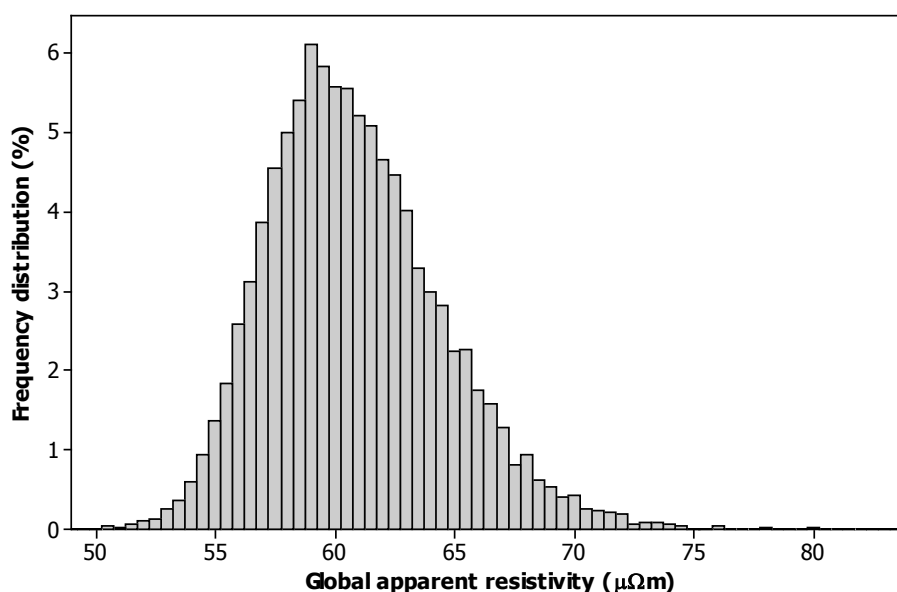


Figure 8. Global apparent resistivity distribution of Alouette population.

3.3. Identification of faulty anodes using a multivariable approach

One of the major objectives of the industrial MIREA device is to estimate the quality of each anode in order to reject anodes having critical deficiencies leading to premature anode failures in the pots or leading to excessive energy consumption. As shown in Section 3.1, anodes having deficiencies can easily be observed due, for example, to the presence of “sawtooth” patterns. However, establishing a quality ranking for these anodes remains arbitrarily, if relying on the averaged analysis of Section 3.1.

One standard and straightforward approach is the use of a multivariate analysis [4] such as the principal component analysis (PCA) with the Mahalanobis distance in order to classify the anode in multiple quality categories. The PCA treatment allows exploratory data analysis by discarding the noise in the initial data set. This facilitates visualization and data interpretation. Briefly, the PCA analysis transforms the MIREA data space, which includes 28 highly correlated “mV” measures into a set of uncorrelated variables called principal components. These components are the eigenvector of the covariance matrix for the initial 28 “mV” measures. The first principal component explains the highest amount of variability in the data set, whereas the latest components explain the lower variability, which is often associated to noise. The Mahalanobis distance is the distance between a data point representing the anode “mV” fingerprint and the multivariate space's centroid (fingerprint of the averaged anode). This distance is used to identify outliers. The higher is the Mahalanobis distance for a specific anode, the higher the “mV” fingerprint of this anode is from the averaged fingerprint of the population. In simple terms, it is an indicator of how different the anode is from the averaged anode. Anodes with a high Mahalanobis distance can be attributed to defective and mediocre anodes. Indeed, the “mV” fingerprint of a good anode does not differ greatly from the averaged fingerprint, since, as explained earlier, there is a physical limit to producing low resistive anodes. However, mediocre anodes are not constrained by a physical limit and can reach high resistance values. They can, thus, be very different from the averaged anode fingerprint.

Figure 8 shows the Mahalanobis distribution of the Alouette population. The figure ordinate is set to a normal scale. This distribution encompasses more than 10 000 anodes. As one can see, more than 95% of the anode population is within a Mahalanobis distance of 7 units. The rest of the population is found within a range of 7 and 40 units. The blue and red points represent respectively the defective and fair anodes presented in Figures 4, 5 and 6 of Section 3.1.

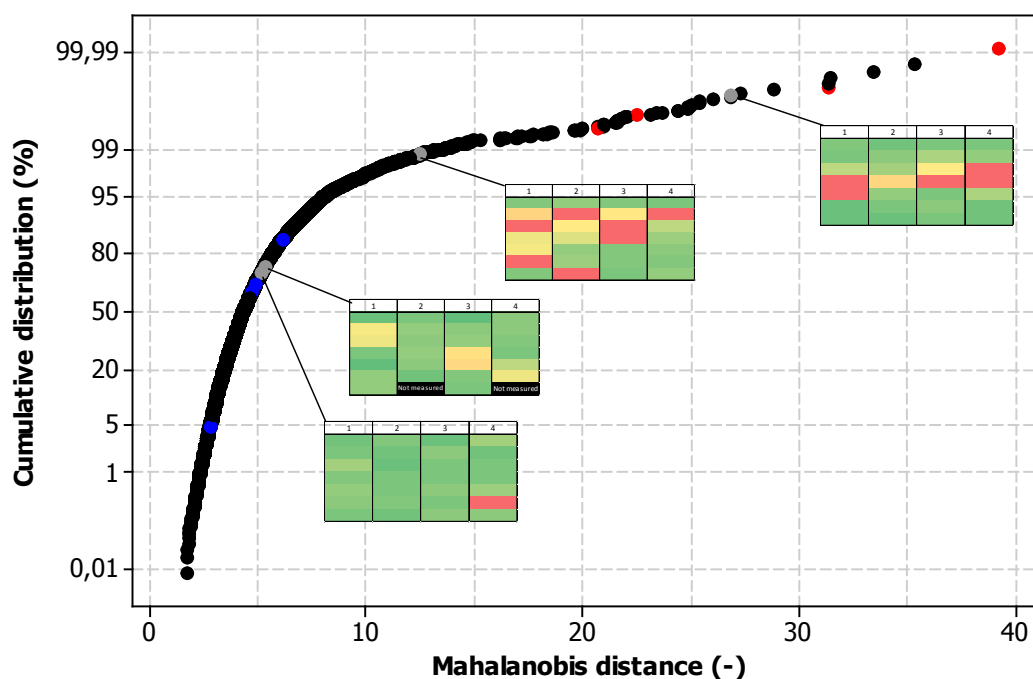


Figure 8. Mahalanobis distribution and core resistivity results from the drilling campaign.
Colormap thresholds: 48 $\mu\Omega\text{m}$ (green); 65 $\mu\Omega\text{m}$ (yellow); 200 $\mu\Omega\text{m}$ / broken subcores (red); too small subcores to be measured (black).

Figure 8 also shows cored resistivity results of four anodes that were specially selected to represent the variability within the Alouette population: two of them were considered as mediocre, the two others, as fair. These anodes were measured by the MIREA device and then collected back for a resistivity drilling campaign. Four back-to-back cores were withdrawn from each selected anode. These cores were located near each MIREA measurement columns. The cores were divided into seven subcores to conduct standard resistivity measurements along the anode height. The resistivity results were translated into colormap tables, as seen in Figure 8. A table section turning to the red scale indicates a highly resistive subcore sample, while a section turning to green represents a normal resistive subcore. It can be seen that the two selected mediocre anodes showed highly resistive regions with the drilling campaign. With the MIREA analysis, both anodes were found in the upper 1.25 % Mahalanobis distribution tail. This position in the distribution identifies them as non-standard anodes. One of these two anodes is among the ten most unusual anodes of the 10 000 anode population. This is explained by the presence of an important horizontal crack in the middle section of the anode. As for the fair anodes, both of them are within the 70 and 80 % centile of the distribution

The Mahalanobis analysis of Figure 8 is a clear indication of the MIREA ability to identify anodes having defective properties. It must be added that comparisons between the other MIREA results and the surface observations on 20 selected anodes, representing a wide

spectrum of the Alouette population, were also performed and showed similar capacities (analysis not included in this paper).

4. Conclusion

This paper presented a preview of the capacity of this on-line process technology by summarizing the resistance measurements of more than 10 000 anodes produced between June and August 2015. Alouette smelter is on track to fully characterize the electrical performance of their anode population and control more efficiently the anode production process. It must be added that it was the first time, in prebaked aluminium technology history, that such a large batch of anodes was individually characterized. This achievement represents a major breakthrough in baked anode quality control.

The standard Mahalanobis analysis presented in this paper allowed an initial classification of the anode resistance quality. Other algorithms are now being set up to identify and reject anodes having specific deficiencies leading to premature anode failures in pots or leading to excessive energy consumption. These algorithms will continue to be refined as Alouette obtains more data on the anode performance during the electrolysis cycle.

5. Acknowledgements

The authors wish to acknowledge the numerous contributors of the Rio Tinto Reduction R&D team for their ingenuity and tenacity which resulted in the development of the MIREA device. Finally, the precious help of Mrs. S. de Moor and Mrs. A. Simard in reviewing this paper is greatly appreciated.

6. References

1. M.-J. Chollier-Brym, D. Laroche, A. Alexandre, M. Landry, C. Simard, L. Simard and D. Ringuette, "New Method for Representative Measurement of Anode Electrical Resistance", *Light Metals*, (2012), 1299-1302.
2. ISO 11713, "Carbonaceous Materials used in the Production of Aluminium - Cathode Blocks and Baked Anodes - Determination of Electrical Resistivity at Ambient Temperature", International Organization for Standardization, (2000).
3. G. Léonard, G. Guérard, D. Laroche, J.-C. Arnaud, S. Gourmaud, M.-J. Chollier and Y. Perron, "Anode Electrical Measurements: Learning and Industrial On-Line Measurement Equipment Development", *Light Metals*, (2014), 1269-1274.
4. K. Esbensen, "Multivariate Data Analysis: In Practice: An Introduction to Multivariate Data Analysis and Experimental Design", 5th Edition, CAMO, Norway, 2004, 598 pages.